Saturation of Plasma Microturbulence by Damped Eigenmodes

P.W. Terry,[1] D.R. Hatch,[1] W.M. Nevins,[2] F. Jenko,[3] F. Merz,[3] J.-H. Kim,[1] and K. Makwana[1]

1) Department of Physics, University of Wisconsin-Madison, Madison, Wisconsin 53706
2) Lawrence Livermore National Laboratory, Livermore, California
3) Max Planck Institute for Plasma Physics, Garching, Germany

E-mail: pwterry@wisc.edu

Abstract: Tokamak microturbulence is shown to saturate by transferring energy to damped eigenmodes in the wavenumber range of the instability rather than by the usual energy cascade to dissipated small scales. This is established for the gyrokinetic formulation of ion temperature gradient turbulence by projecting the saturated nonlinear state onto complete basis sets, including the linear eigenmodes of the gyrokinetic operator and the basis of a proper orthogonal decomposition. These projections are applied to nonlinear initial value simulations of the gyrokinetic code GENE. For the CYCLONE base case hundreds of damped eigenmodes are excited to significant levels. Calculation of energy dissipation rates shows that the modes excited produce an energy sink in the wavenumber range of the instability that at certain scales dissipates energy faster than the instability injects energy. Proper orthogonal decomposition establishes that prompt access to dissipation in the form of weakly interacting dissipative eigenstates creates an equipartition of a form of dissipation rate in each orthogonal mode. There are indications that damped eigenmodes impart their frequencies to the frequency spectrum at fixed wavenumber and account for the large linewidth observed in simulation and experiment. Zonal flows, while excited to large amplitude, dissipate little energy compared to other damped eigenmodes. Analysis of energy flow shows that damped eigenmodes provide the energy sink for saturation, but fluctuation levels are lower when the energy passes through zonal flows to the damped eigenmodes than when energy bypasses zonal flows. The secondary Kelvin-Helmholtz instability that breaks up the structure of the electron temperature gradient instability is found to be a dissipative structure through excitation of damped eigenmodes. Damped eigenmodes also saturate turbulence in other models of plasma microturbulence, including trapped electron mode, Rayleigh-Taylor, resistive interchange mode, and collisional drift wave turbulence.

1. Introduction

The physics of saturation of plasma microturbulence in tokamaks is an open and unresolved issue, and unlike hydrodynamic turbulence, has an important effect on energy containing scales. In high Reynolds number hydrodynamic turbulence the physics of the viscous energy sink that enables a steady state has negligible effect on dynamics in the inertial range, because the dissipation is confined to a highly separated small-scale range. Dynamics at large scales is dominated by conservative, scale-independent spectral transfer. This paradigm has been assumed to apply to plasma turbulence as well, leading to the notion that transport and other properties dominated by the energy containing scales are not sensitive to the physics of saturation. We show here that fluctuation levels, transport, and other observable consequences of the turbulence are governed, not just by the driving instability, but by the mechanism that saturates the instability and dissipates the fluctuation energy.

The preceding statement is based on evidence, presented here, that saturation of plasma instabilities does not occur primarily through an energy transfer to small scales where it is dissipated but by nonlinearly exciting eigenmodes that are damped for every wavenumber in the spectrum. Damping of these eigenmodes for wavenumbers in the instability range dissipates most of the energy of the instability before it reaches small scales. This is a novel process relative to standard paradigms. Driving and dissipation ranges completely overlap, with dissipation peaking in the driving range although it extends outside. In place of the conventional cascade in wavenumber space, with scale invariance in inertial scales, there is transfer to a hyperspace of damped eigenmode manifolds. This hyperspace is infinite in the gyrokinetic formalism and becomes finite only under discretization of the gyrokinetic operator.

This type of saturation mechanism applies to turbulence that is thought to govern tokamak core transport, including ion and electron temperature gradient turbulence (ITG and ETG) [1]-[2], and trapped electron mode turbulence [3]. It also applies to a variety of other types of turbulence, including Rayleigh-Taylor turbulence, resistive interchange turbulence, collisional drift wave turbulence, scrape-off layer turbulence, and microtearing turbulence [4]. This paper provides a summary of what is presently known about this type of saturation mechanism, including how gyrokinetic and fluid descriptions affect the overall picture.

2. Gyrokinetic Modeling of Ion Temperature Gradient Turbulence

Gyrokinetic simulation of ITG turbulence saturates to a converged spectrum even when scales beyond the region of positive growth are not well resolved. This is in contrast to high-Reynolds-number hydrodynamic turbulence, in which the range of dynamically important scales beyond the scales of energy input is so large that no simulation can resolve it. This difference, which has had no prior explanation, is consistent with saturation by damped eigenmodes in the wavenumber range of the instability. To examine the role of damped eigenmodes in saturation of ITG turbulence, an eigenmode solver developed for the gyrokinetic code GENE [5] has been used to project the saturated turbulent state as evolved from initial value simulation onto the compete linear basis set of the discretized gyrokinetic operator. The standard resolution of the CYCLONE base case yields over 10^4 damped eigenmodes, of which there are at least several hundred that are excited to significant amplitudes. Figure 1 shows the frequency, growth rate, and amplitude of a selection of eigenmodes, all with the same wavevector, in the unstable range. The single unstable mode is included. The modes selected are nearly orthogonal. The amplitude, in conjunction with the damping rate, gives a sense of the magnitude of energy dissipated by each mode. It is clear from Fig. 1 that many damped eigenmodes contribute to the saturation of the instability.

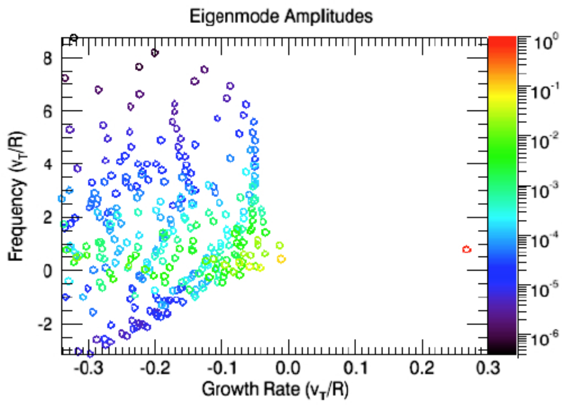

Fig. 1. Amplitude (color) as a function of growth rate and frequency for 315 of the least damped eigenmodes of the linearized gyrokinetic operator for a Fourier wavenumber k_y = 0.3 and k_x = 0.0 in the region of instability.

To determine the rate at which damped eigenmodes dissipate energy, the dissipative (non conservative) terms of the gyrokinetic operator are used to construct a finite-amplitude-induced fluctuation dissipation rate shown in Fig. 2. The “dissipation” rate of the most unstable eigenmode (blue curve) is positive, indicating energy input over the wavenumber range of the instability ($0 < k_y\rho_s<0.7$). The total dissipation rate (black curve), which includes the effect of damped eigenmodes, becomes negative for $k_y\rho_s < 0.1$ and $k_y\rho_s > 0.4$, indicating that damped eigenmodes remove energy in those scales faster than it is injected by the instability. Damped eigenmodes also remove energy in the scales $0.1 < k_y\rho_s < 0.4$, but at a rate that is slower than the instability input rate. In the range $0.15 < k_y\rho_s < 0.25$ there is a second linearly unstable eigenmode. There is also subcritical instability associated with the excitation of stable eigenmodes. These increase the energy input rate above that of the most unstable eigenmode. The dissipation rate attributable to everything but the most unstable eigenmode (red curve) is thus slightly positive for $0.15 < k_y\rho_s < 0.25$, is strongly negative everywhere else, and becomes constant above $k\rho_s = 0.4$.

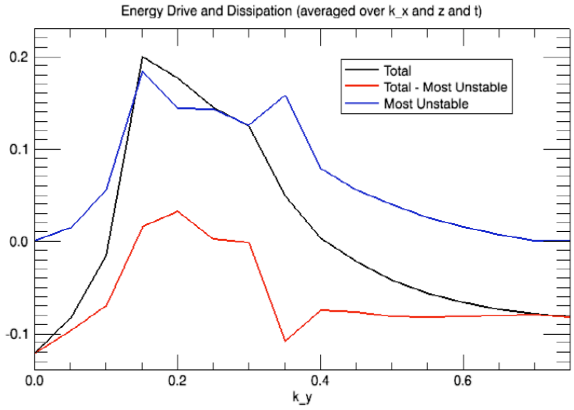

Fig. 2. Energy input rate of the unstable eigenmode (blue), stable eigenmodes (red) (whose mostly negative value corresponds to energy damping) and net rate of the two combined (black) across the wavenumber range of the instability.

It is instructive to determine how the rates represented in Fig. 2 are apportioned into contributions from the cross correlation of the heat flux, collisions, and numerical dissipation. Under such a breakdown the energy evolves according to

$$\left.\frac{\partial E_k}{\partial t}\right|_{NC} = C_k + D_k + N_k\ , \tag{1}$$

where NC indicates that only non conserving terms are included in the evolution (the conservative nonlinearity is excluded). Here $C_k = \int dv_\parallel d\mu\, \pi\, n_0 T_0 B_0 \times (v_\parallel^2 + \mu B_0)\omega_T g^* ik_y\overline{\phi}$ is a correlation of potential and gyro-center ion distribution function g that is proportional to heat flux, D_k represents collisional dissipation, and N_k is numerical dissipation. The energy is given by $E = \int dv_\parallel d\mu B_0\, (n_0 T_0 / F_0)|g|^2 + H(k_\perp)|\phi|^2$, where H is a function of perpendicular wavenumber. For the Cyclone base case the contributions to Eq. (1) have been evaluated for each mode of a proper orthogonal decomposition (POD) [6]. The mode with the largest singular value (largest contribution to the turbulent dynamics) is essentially the unstable eigenmode. It has C_k positive and much larger than $D_k + N_k$. This is consistent with the ITG instability drive. The remaining modes are damped. Those with larger singular values can have sizable C_k, but C_k can be either positive or negative depending on the mode. Averaged over singular values, C_k is very small. This is consistent with earlier work on the cross phase, which showed that its mean value did not deviate significantly from the linear value (given by the unstable eigenmode) but the standard deviation was very large [1]. In contrast $D_k + N_k$ is systematically negative for the damped modes and large compared to the average value of C_k. We conclude that for the Cyclone base case of ITG turbulence, the damped eigenmodes saturate the instability primarily through collisional damping. This damping is concentrated in large scales for x and y (small values of k_x and k_y). In contrast the damping occurs in both large and small values of k_x and for parallel velocities that are both small and large.

The damped modes satisfy a condition that asymptotically corresponds to equipartition of a form of dissipation rate of each orthogonal mode. This is consistent with a gas of weakly interacting eigenstates in which dissipation rates balance equipartitioned energy transfer rates. This condition, which can be formulated statistically using a Gibbs distribution, replaces the scale invariance of large-Reynolds-number hydrodynamic turbulence as the organizing principal for excitation among available states in plasma microturbulence. Analysis of dissipation range spectra for constant damping under advective nonlinearities yields power law spectra, as observed in simulation. There is also some evidence that anomalously broad frequency spectra at fixed k, as observed in simulation and experiment [7], reflect frequencies of damped eigenmodes [1]. Zonal flows are excited to finite levels but dissipate little energy relative to damped eigenmodes that are not zonal flows. While analysis of energy flow shows that damped eigenmodes provide the energy sink for saturation, fluctuation levels are lower when the energy passes through zonal flows to the damped eigenmodes than when energy bypasses zonal flows. This is quite different from the role postulated in the zonal flow paradigm, which assumes that transfer to small scales enhanced by zonal flow shear saturates the turbulence [8].

3. Damped Eigenmodes in Electron Temperature Gradient Turbulence

Eigenmode projection has been used in analysis of the numerical solution of ETG turbulence saturation. We consider an electromagnetic model for ETG turbulence that includes evolution equations for vorticity, electron pressure, and the parallel component of the magnetic vector potential [9]. The ETG instability is known to undergo transition to the turbulent state through a process that involves a secondary Kelvin-Helmholtz (KH) instability that breaks up the primary ETG structure [10]. It is found that the secondary instability and the ensuing nonlinear evolution are associated with strong excitation of damped eigenmodes and strong energy dissipation. Figure 3 shows the nonconservative energy evolution rates. In Fig. 3a, the rates are normalized by energy to yield growth rates.

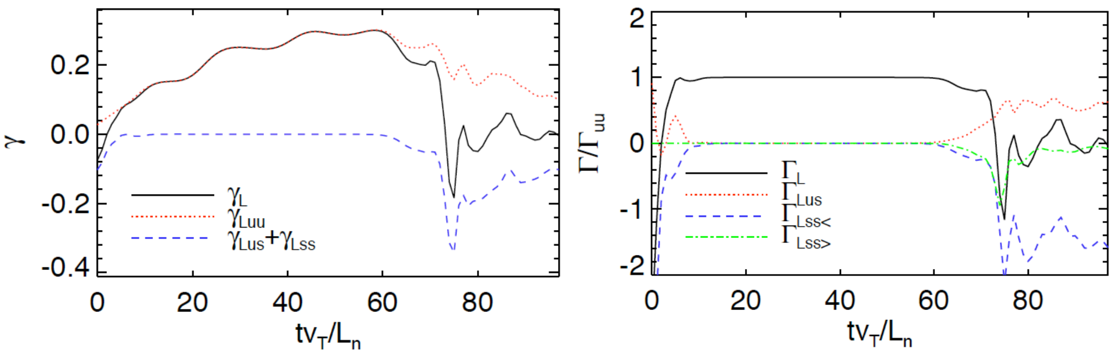

Fig. 3. Energy evolution rates showing contributions from unstable and stable eigenmodes.

The growth rate γ_L represents the total energy input summed over wavenumber. It is positive during the linear growth phase when $tv_T/L_n < 60$. In saturation it oscillates around zero because it includes both instability drive and the damping that produces saturation, which must balance for a steady state. The total energy input is closely matched by the energy input of the unstable eigenmodes during the linear phase. Energy input by damped eigenmodes is zero during this phase, but after saturation it is negative and roughly opposite the still positive energy input by unstable eigenmodes. This indicates that damped eigenmodes saturate the instability. Saturation is not accomplished by transfer to the large viscously damped wavenumbers of the unstable mode. Were this the case, the red trace would drop to zero after $tv_T/L_n < 60$, and the blue trace would never reach negative values. Figure 3b, which has energy evolution rates Γ that have not been normalized to yield growth rates, shows that it is the damped eigenmodes in the wavenumber range of the instability that provide saturation. The green trace represents damped eigenmodes in small scales beyond the instability range, while the blue trace represents damped modes in the instability range. There is a transient at the onset of the nonlinear state in which small scales dissipate fluctuation energy, but thereafter the damping in small scales is nearly zero and damping is concentrated in large scales. From analysis of individual nonlinearities, it is found that the transient corresponds to a brief period of strong vorticity advection associated with the KH instability. After the transient vorticity advection is weak compared to pressure advection. We conclude that the KH secondary instability is not solely an inertial structure that conducts instability energy to small scales where it can be viscously dissipated. Instead it is a dissipative structure whose large scales access the damping of damped eigenmodes.

Moreover, whereas the KH instability operates transiently, damped eigenmodes through pressure advection operate continuously to provide saturation throughout the nonlinear state.

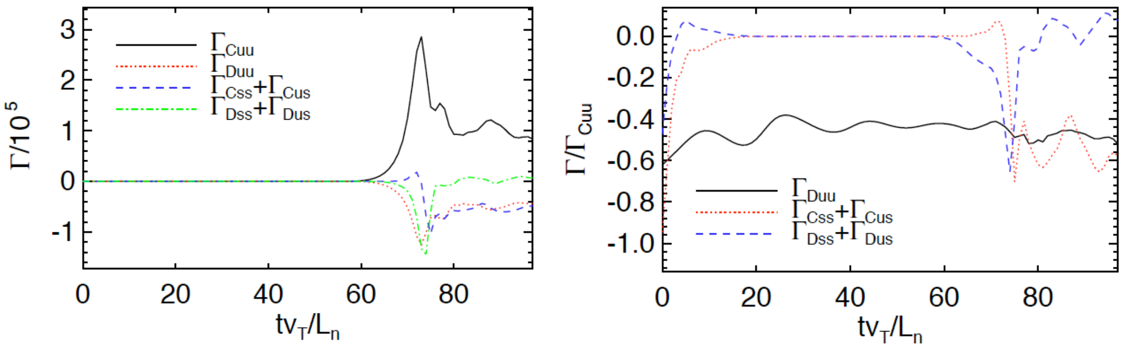

Fig. 4. Contribution to energy evolution from cross phase and collisions.

Figure 4 breaks energy evolution rates into the components associated with cross phase (C) and collisional dissipation (D). In Fig. 4a, collisional damping associated with damped eigenmodes, represented by the green trace, is significant only during the transient. After the transient the energy injected by the instability is balanced by fluctuation dissipation from the cross phase associated with damped eigenmodes (blue trace) and collisional dissipation in the unstable eigenmode (red trace). The latter is seen from Fig. 4b to be intrinsic to the mode structure of the unstable eigenmode. In this figure, the collisional dissipation in the unstable eigenmode is normalized to the unstable cross correlation that drives instability. The trace is nearly constant, indicating a residual collisional damping that is overcome by the unstable cross phase. Figure 4 illustrates a striking difference between damped mode saturation in ETG and the Cyclone base case of ITG. In the latter damped modes saturate the linear instability primarily though collisions, while in the former it is through the cross correlation. As shown in the next section, damped eigenmodes in other types of fluid turbulence also saturate the instability, principally through the cross correlation.

4. Damped Eigenmodes in Fluid Turbulence

The preceding sections and prior work [1]-[3] have dealt with core turbulence in tokamaks. We show that saturation by damped eigenmodes is widespread in unstable plasmas and not peculiar to some restricted set of physical processes, parameter regimes, or models. To do this we study saturation in two-fluid models for trapped electron turbulence (TEM) [3], Hasegawa-Wakatani turbulence [11], Rayleigh-Taylor turbulence [12], ITG [13], microtearing turbulence [14], thermally driven microtearing turbulence [15], thermally driven drift waves [16], and ionization driven drift waves [17]. These models include electrostatic and magnetic fluctuations, they span regimes in temperature from hot to cold, in trapping physics from trapped to untrapped, in field line configuration from closed to open, and in discharge locale from core to scrape-off layer.

All of these models have regimes in which damped eigenmodes provide the dominant saturation mechanism. For TEM and Hasegawa-Wakatani turbulence this regime is the weakly collisional regime (sometimes labeled collisionless) and the hydrodynamic regime respectively. In these regimes dissipative processes in the diagonal terms of the original model are weak compared to off-diagonal terms. The diagonal terms enter the energy as squared amplitudes, while the off-diagonal terms enter as amplitude cross correlations. The off-diagonal terms are complex because of diamagnetic frequencies or similar physics associated with equilibrium gradients. This is true for most of the models – saturation is dominated by damped eigenmodes when gradient instability drive from cross correlations is strong.

However, the scrape-off layer models are driven by negative dissipation in the diagonal terms and are therefore quite different. Nonetheless they too have regimes where the damped eigenmode saturates the instability. A feature of quadratic dispersion (which does not carry over to higher order) is that very near instability threshold the damped eigenmodes are so heavily damped that saturation is accomplished through the conventional cascade to small scales.

The dominance of the damped eigenmode in saturating the instability in all of these models is well predicted by an eigenmode activity threshold parameter [17] given by

$$P_t = \frac{D_1(C_2 + C_3)}{C_1^2(2 - \gamma_2/\gamma_1)} , \tag{2}$$

where γ_2 is a damping rate of the damped eigenmode, γ_1 is the growth rate of the instability, C_1 is the coupling strength for transfer to high k on the manifold of the unstable eigenmode, D_1 is the coupling strength for transfer to a damped mode from two unstable modes, and $C_2 + C_3$ are coupling strengths for transfer away from the unstable mode to damped eigenmodes. All quantities in P_t depend on wavenumber and are evaluated in the wavenumber range of the instability. P_t is intended as a rough measure of the importance of damped eigenmodes in saturation. When its value is order unity damped eigenmodes are important in saturation. When it is much smaller than unity, it is expected that saturation will occur through transfer on the unstable manifold to collisionally damped wavenumbers at high k. The parameter P_t is strongly sensitive to the ratio γ_2/γ_1. When the ratio becomes much larger than unity, the parameter value decreases. Simulations show that damped eigenmode activity weakens as P_t decreases. However, even when γ_2/γ_1 becomes quite large, the damped eigenmode continues to be the primary saturation energy sink. Figure 5 shows the ratio of the rate of energy dissipation in the damped mode to the rate of energy injection by the unstable mode as a function of γ_2/γ_1. The simulation is for trapped electron mode turbulence. This ratio remains close to order unity as γ_2/γ_1 ranges between 1 and several hundred. Only when γ_2/γ_1 becomes larger several hundred does energy dissipation by the damped mode begin to fall out of balance with energy input. This is due in part to the fact that the coupling ratio $D_1(C_2 + C_3)/C_1^2$ is larger than unity. However it is also the case that the damped mode remains important as γ_2 increases because the damped eigenmode is directly accessed in every triad, whereas the damping on the unstable manifold requires a cascade through a series of triads.

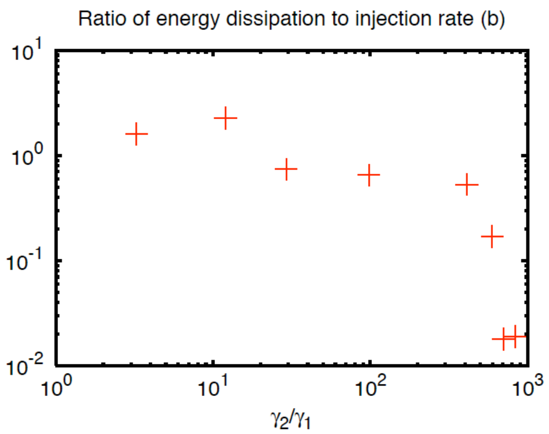

Fig. 5. Ratio of energy dissipation to injection rate as a function of damping to growth rate ratio for trapped electron mode turbulence.

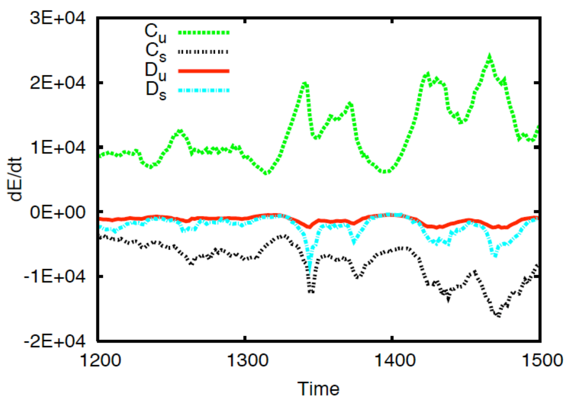

Fig. 6. Attribution of energy rate (injection or dissipation) to cross-correlation and collisional terms associated with unstable and damped modes in ITG turbulence.

Like ETG, damped eigenmodes in the two-field fluid models have a significant and systematic effect on the cross correlation, which provides the largest single sink of energy for saturation. This is shown in Fig. 6, which breaks the energy rate of change into components that depend on the cross correlation between unstable mode amplitudes (C_u), components that depend on the cross correlation with stable mode amplitudes (C_s), and components that depend on collisional dissipation (D_u and D_s). The simulation is for ITG turbulence. Like ETG, C_s is the largest offset to the instability drive.

5. Conclusions

We have shown that damped eigenmodes are a pervasive and significant player in the saturation of instability-driven plasma turbulence. This has been verified for many types of turbulence and is true whether there are many damped eigenmodes or one. The statement applies to both kinetic and fluid systems. Indeed, it appears that when there is a single damped eigenmode the system channels fluctuation energy to that mode. When there are many it si channeled to all modes under an equipartition arrangement. Reduced fluid models thus behanve qualitatively like low resolution kinetic models in the saturation by damped eigenmodes. Damped eigenmodes dissipate fluctuation energy through cross correlations that relate to transport fluxes and through collisional terms. For fluid models the former dominate, while for CYCLONE-base-case ITG the latter dominate. The origin of this difference, which has bearing on the goodness of the quasilinear transport approximation, is not understood but will be studied in future work. In both fluid models and CYCLONE-base-case ITG the damped eigenmodes provide a sink of energy in the same scales as the fluctuation drive. With no scale separation between drive and damping in instability-driven plasma turbulence, fluctuation levels and transport can only be properly treated if the saturation mechanism is as well understood as the driving instability.

A number of key aspects of damped eigenmode saturation have been studied only cursorily. These include the mechanism by which zonal flows lower fluctuation levels fixed by damped eigenmode saturation. They include the mode coupling process responsible for observed equipartition of a form of dissiption rate across a POD spectrum. They include study of the effect of damped eigenmodes on the frequency spectrum at fixed k, the parallel parity properties of damped eigenmode fluctuation structures and their effect on stochasticity, and phase-space characteristic of energy transfer to damped eigenmodes. These processes are all under study and will be described in greater detail in the future.

Work supported by USDOE

[1] D.R. Hatch, et al., Phys. Plasmas **16**, 022311 (2009).

[2] J.-H. Kim and P.W. Terry, Phys. Plasmas **17**, (2010), in press.

[3] D.A. Baver, et al., Phys. Plasmas **9**, 3318 (2002).

[4] K. Makwana and P.W. Terry, Bull. Amer. Phys. Soc. **54**, No. 15, 40 (2009).

[5] F. Jenko, et al., Phys. Plasmas **7**, 1904 (2000).

[6] D. del-Castillo-Negrete, D.A. Spong and S.P. Hirshman, Phys. Plasmas **15**, 092398 (2006).

[7] Morgan W. Shafer, Ph.D. Thesis, University of Wisconsin, 2009.

[8] P.H. Diamond, et al., Plasma Phys. Controlled Fusion **47**, R35 (2005).

[9] W. Horton, B.G. Hong, and W.M. Tang, Phys. Fluids **31**, 2971 (1988).

[10] W. Dorland, F. Jenko, M. Kotschenreuther, and B.N. Rogers, Phys. Rev. Lett. **85**, 5579 (2000).

[11] A. Hasegawa and M. Wakatani, Phys. Rev. Lett. **50**, 682 (1983).

[12] A. Das, et al., Phys. Plasmas **4**, 1018 (1997).

[13] C. Holland, et al., Nucl. Fusion **43**, 761 (2003).

[14] A.B. Hassam, Phys. Fluids **23**, 38 (1980).

[15] G.G. Craddock and P.W. Terry, Phys. Fluids B **3**, 3286 (1991).

[16] A.S. Ware, et al., Phys. Fluids B **4**, 102 (1992).

[17] A.S. Ware, et al., Phys. Fluids B **4**, 877 (1992).

[18] P.W. Terry, D.A. Baver, and S. Gupta, Phys. Plasmas **13**, 022307 (2006).